

STRUCTURE
OF INORGANIC COMPOUNDS

A Novel Cesium Pentaborate
with Ribbon-Type Anionic Radical

L. V. Shvanskaya^{a,*} and A. V. Sapegina^a

^aMoscow State University, Moscow, 119992 Russia

*e-mail: lshvanskaya@mail.ru

Received March 22, 2018; revised April 9, 2018; accepted May 10, 2018

Abstract—A novel hydrated cesium hydroxypentaborate is synthesized from boric acid flux at 180°C, and its crystal structure is determined by X-ray diffraction. The compound crystallizes in the triclinic system, sp. gr. $P\bar{1}$, with the parameters $a = 7.8107(5)$ Å, $b = 9.1929(8)$ Å, $c = 12.3553(11)$ Å, $\alpha = 98.98(1)^\circ$, $\beta = 106.32(1)^\circ$, $\gamma = 91.10(1)^\circ$, $V = 839.1(1)$ Å³, $Z = 4$. The structure is refined to $R_1 = 5.8\%$ with anisotropic displacement parameters for all nonhydrogen atoms, with allowance for the non-merohedral twinning by a twofold axis coinciding with the b axis. The twin components were 0.546(1) and 0.454(1). The features of the hydrogen bonds in $\text{Cs}[\text{B}_5\text{O}_7(\text{OH})_2] \cdot 0.5\text{H}_2\text{O}$ are analyzed in comparison with isostructural rubidium analogue. The unit-cell parameters a and c of $A[\text{B}_5\text{O}_7(\text{OH})_2] \cdot 0.5\text{H}_2\text{O}$ pentaborates are found to systematically increase with an increase in the radius of A cation in the $\text{NH}_4 \rightarrow \text{Rb} \rightarrow \text{Cs}$ series; the small variation in the b parameter is due to the rigidity of the pentaborate chains elongated along this direction.

DOI: 10.1134/S1063774519010243

INTRODUCTION

The anion radicals in the crystal structures of six cesium pentaborates that have been studied to date are formed from blocks consisting of one central BO_4 tetrahedron and four triangles, sharing vertices with it. Pentaborate anionic radicals are isolated in hydrated polymorphic α [1] and β [2] modifications of $\text{Cs}[\text{B}_5\text{O}_6(\text{OH})_4] \cdot 2\text{H}_2\text{O}$. The main difference in the crystal structures of polymorphs is that the boron atom (centering the oxygen tetrahedron) occupies a special position in the β phase: it is located on a two-fold axis. Therefore, only three boron atoms are independent in the $[\text{B}_5\text{O}_6(\text{OH})_4]$ block. At the same time, there are five independent boron polyhedra in the α modification. In this case, boron triangles and tetrahedra obey the following scheme: $5 : 2(2\Delta + 0.5T)$ and $5 : (4\Delta + 1T)$ for the β and α modifications, respectively. Four polymorphic modifications (α , β , γ , and δ) of anhydrous pentaborate CsB_5O_8 have framework structures, differing in the configurations of the channels containing cesium cations. Among the known alkali metal pentaborates, we should select isostructural compounds of rubidium and ammonium, $A[\text{B}_5\text{O}_7(\text{OH})_2] \cdot 0.5\text{H}_2\text{O}$ [3, 4], which were obtained under hydrothermal conditions and by flux synthesis. Their crystal structures contain ribbon motifs composed of pentaborate blocks, which are topologically identical to the blocks in the structure of mineral larderellite $\text{NH}_4[\text{B}_5\text{O}_7(\text{OH})_2] \cdot \text{H}_2\text{O}$ [5]. Note that other hydrated alkaline pentaborates (all nezo- ones, sborgite $\text{Na}[\text{B}_5\text{O}_6(\text{OH})_4] \cdot 3\text{H}_2\text{O}$ [6], santite $\text{K}[\text{B}_5\text{O}_6(\text{OH})_4] \cdot$

$2\text{H}_2\text{O}$ [7], and ammonioborite $(\text{NH}_4)_2[\text{B}_5\text{O}_6(\text{OH})_4]_2 \cdot \text{H}_2\text{O}$ [8], as well as Rb and Cs ramanites $A[\text{B}_5\text{O}_6(\text{OH})_4] \cdot 2\text{H}_2\text{O}$ [9], found in melt and fluid inclusions of pegmatite quartz) are also crystallized under natural conditions. Based on the similarity between their diffraction patterns and the diffraction patterns of synthetic analogues, isostructurality of Rb ramanite and santite (sp. gr. *Aba2*) was established; Cs ramanite is isostructural to the β modification of synthetic $\text{Cs}[\text{B}_5\text{O}_6(\text{OH})_4] \cdot 2\text{H}_2\text{O}$ (sp. gr. *C2/c*).

The interest in hydrated pentaborates is caused by their potential application as laser frequency converters. In particular, nonlinear optical properties were found for polar representatives of the $\text{Me}[\text{B}_5\text{O}_6(\text{OH})_4] \cdot 4\text{H}_2\text{O}$ family, $\text{Me} = \text{K}$ [10], Cs, NH_4 [11].

In this paper, we report the results of the synthesis and X-ray diffraction analysis of a novel hydrated cesium pentaborate with a ribbon-type anionic radical.

EXPERIMENT AND STRUCTURE
REFINEMENT

Colorless transparent crystals of the novel compound with an elongated lamellar habit were obtained from boric acid (H_3BO_3) flux when studying the phase formation in the multicomponent system $\text{Cs}-\text{Cu}-\text{P}-\text{B}-\text{O}$. The initial agents $\text{H}_3\text{BO}_3 : \text{CsH}_2\text{PO}_4 : \text{CuO}$, taken in a molar ratio of 10 : 1 : 2, were carefully ground and placed in a autoclave lined with Teflon. Heating was performed to 180°C, and the melt was kept for 7 days, with subsequent cooling to room tem-

perature. Crystals were mechanically extracted from the gray-blue mass. Rounded dark blue and dark gray particles with metallic luster were identified by X-ray diffraction analysis as amorphous phases. Based on the preliminary X-ray diffraction data, the unit-cell parameters of isolated crystalline phase were found to be $a = 7.7999(5) \text{ \AA}$, $b = 9.1767(9) \text{ \AA}$, $c = 12.3342(11) \text{ \AA}$, $\alpha = 98.985(8)^\circ$, $\beta = 106.344(7)^\circ$, $\gamma = 91.099(7)^\circ$, and $V = 837.1 \text{ \AA}^3$. Qualitative X-ray spectroscopic analysis of single crystals (Jeol JSM-6480LV, energy-dispersive attachment INCA 350) showed the presence of Cs, B, and O atoms in their composition. Based on the data of preliminary phase study and chemical analysis, it was suggested that the novel compound is a cesium analog of alkaline pentaborates $\text{Rb}[\text{B}_5\text{O}_7(\text{OH})_2] \cdot 0.5\text{H}_2\text{O}$ and $\text{NH}_4[\text{B}_5\text{O}_7(\text{OH})_2] \cdot 0.5\text{H}_2\text{O}$, which were synthesized previously under soft hydrothermal conditions and by the flux method [3, 4], respectively. Further solution and refinement of the compound structure confirmed this suggestion.

An experimental set of diffraction reflection intensities was collected on an X-ray diffractometer Xcalibur S (Oxford Diffraction) with a two-dimensional CCD detector at room temperature. The recorded reflection intensities were corrected using the diffrac-

tometer software taking into account the Lorenz and polarization factors. An analysis of the experimental set of X-ray reflections using the CrysAlisPro software package [12] showed the crystal to be a non-merohedral twin, whose components are linked by a twofold pseudoaxis oriented along the [010] direction. Reflections from different twin components were separated in a new set and empirical absorption correction was introduced. All calculations were performed within the WinGX 32 software package [13]. The atomic scattering curves and anomalous dispersion corrections from [14] were applied. The crystal structure was solved by direct methods in the sp. gr. $P\bar{1}$ and refined (using the SHELX program [15]), based on the intensities separated for each twin component in the reflection file HKLF5, to the $R = 0.0586$ (for 7529 unique reflections with $I > 2\sigma(I)$) with anisotropic displacement parameters for all non-hydrogen atoms. The sites of four unique H atoms forming hydroxyl groups and two sites belonging to the water molecule were revealed in Fourier difference maps and refined in the isotropic approximation. An empirical value of 0.90 \AA was assigned to the O–H bond length. The main crystallographic characteristics, details of the X-ray experiment, and results of structure refinement for the novel cesium pentaborate are listed in Table 1. The

Table 1. Crystallographic characteristics, details of the X-ray experiment, and the structure refinement parameters for $\text{Cs}[\text{B}_5\text{O}_7(\text{OH})_2] \cdot 0.5\text{H}_2\text{O}$

<i>M</i>	341.996
Symmetry, sp. gr., <i>Z</i>	Triclinic, $P\bar{1}$, 2
<i>a</i> , <i>b</i> , <i>c</i> , \AA	7.8107(5), 9.1929(8), 12.3553(11)
α , β , γ , deg	98.98(1), 106.32(1), 91.10(1)
<i>V</i> , \AA^3	839.1(1) \AA^3
<i>D_x</i> , g/cm^3 ; μ , mm^{-1}	2.707; 4.44
Radiation, λ , \AA	$\text{MoK}\alpha$, 0.71069 (graphite monochromator)
<i>T</i> , K	298(2)
Sample size, mm	$0.0796 \times 0.0516 \times 0.0366$
Diffractometer	Xcalibur SCCD
Scan mode	Ω
<i>T_{min}</i> , <i>T_{max}</i>	0.97, 1.00
θ_{max} , deg	30.586
Ranges of indices <i>h</i> , <i>k</i> , <i>l</i>	$-10 \leq h \leq 10$, $-12 \leq k \leq 12$, $-17 \leq l \leq 17$
Number of reflections: measured/observed with $I > 2\sigma(I)$	14576/7529
Refinement technique	Least-squares method on F^2
Number of parameters in refinement	305
Weighting scheme	$1/[\sigma^2(F_o^2) + (0.1P)^2 + 0.00P]$
<i>R₁</i> / <i>wR₂</i>	0.0586/0.1153
Twinning coefficient (BASF)	0.454(1)
<i>S</i>	0.608
$\Delta\rho_{\text{min}}/\Delta\rho_{\text{max}}$, e/\AA^3	$-2.155/1.627$

Table 2. Coordinates of basis atoms and equivalent thermal parameters for the $\text{Cs}[\text{B}_5\text{O}_7(\text{OH})_2] \cdot 0.5\text{H}_2\text{O}$ structure

Atom	x/a	y/b	z/c	$U_{\text{eq}}, \text{\AA}^2$ *
Cs1	0.9925(1)	0.0574(1)	0.2542(1)	0.018(0)
Cs2	0.4011(1)	0.7063(1)	0.2092(1)	0.021(0)
B1	0.4956(15)	0.2422(13)	0.4650(9)	0.011(2)
B2	0.8638(14)	0.8243(13)	0.4378(10)	0.011(2)
B3	0.9135(15)	0.6602(13)	0.0727(10)	0.013(3)
B4	0.9039(16)	0.6578(14)	0.2705(10)	0.016(3)
B5	0.5452(15)	0.2470(13)	0.1040(10)	0.013(2)
B6	0.6777(13)	0.0411(14)	0.4396(9)	0.009(2)
B7	0.7282(16)	0.4757(14)	0.1060(10)	0.015(3)
B8	0.3230(14)	0.0503(14)	0.0669(10)	0.013(2)
B9	0.0813(15)	0.6437(14)	0.4699(10)	0.014(3)
B10	0.5011(15)	0.1382(13)	0.2678(10)	0.009(2)
O1	0.6185(9)	1.1448(8)	0.5124(5)	0.013(2)
O2	1.0508(9)	0.6039(8)	0.3562(6)	0.015(2)
O3	0.7696(9)	0.5338(9)	0.2167(6)	0.016(2)
O4	0.9904(9)	0.7557(8)	0.5137(6)	0.015(2)
O5	0.5960(9)	0.2367(8)	0.2168(6)	0.016(2)
O6	0.6159(9)	0.3522(8)	0.0580(5)	0.014(2)
O7	0.4110(9)	0.1528(8)	0.0275(6)	0.015(2)
O8	0.7917(9)	0.5388(8)	0.0296(6)	0.015(2)
O9	1.2050(10)	0.5731(8)	0.5407(6)	0.017(2)
O10	0.9763(9)	0.7113(8)	0.1854(6)	0.015(2)
O11	0.8230(9)	0.7804(8)	0.3247(6)	0.012(2)
O12	0.1708(12)	0.3856(11)	0.2242(7)	0.037(2)
O13	0.4276(9)	1.2319(8)	0.3503(6)	0.014(2)
O14	0.4471(10)	1.3414(9)	0.5426(6)	0.020(2)
O15	0.9758(9)	0.7275(8)	-0.0014(6)	0.016(2)
O16	0.2046(9)	-0.0486(9)	-0.0134(6)	0.019(2)
O17	0.6271(9)	1.0389(8)	0.3251(5)	0.013(2)
O18	0.7917(9)	0.9431(8)	0.4882(6)	0.013(2)
O19	0.3545(8)	0.0494(8)	0.1799(5)	0.013(2)
H1	0.135(9)	-0.112(8)	0.008(7)	0.08(6)
H2	0.375(9)	1.414(6)	0.522(10)	0.08(6)
H3	0.916(13)	0.671(9)	-0.068(4)	0.04(4)
H4	1.225(19)	0.617(12)	0.614(3)	0.08(6)
H5	0.252(8)	0.319(7)	0.243(12)	0.08(6)
H6	0.116(9)	0.446(9)	0.267(6)	0.06(5)

* Isotropic thermal parameters are given for H atoms.

Table 3. Interatomic distances (\AA) in the $\text{Cs}[\text{B}_5\text{O}_7(\text{OH})_2] \cdot 0.5\text{H}_2\text{O}$ structure

Cs1 nine-vertex polyhedron		Cs2 nine-vertex polyhedron	
O16	2.928(7)	O14	3.067(8)
O4	3.071(7)	O11	3.214(7)
O10	3.153(7)	O6	3.225(6)
O18	3.156(6)	O12	3.247(7)
O11	3.196(7)	O10	3.245(7)
O12	3.207(7)	O3	3.298(7)
O17	3.222(7)	O8	3.368(7)
O _w	3.414(11)	O17	3.395(7)
O5	3.486(7)	O _w	3.481(11)
$\langle \text{Cs1-O} \rangle$	3.204	$\langle \text{Cs2-O} \rangle$	3.282
B1 triangle		B4 tetrahedron	
O13	1.354(12)	O11	1.465(14)
O14	1.356(13)	O10	1.468(14)
O1	1.396(13)	O3	1.472(14)
$\langle \text{B1-O} \rangle$	1.369	O2	1.478(13)
B2 triangle		$\langle \text{B4-O} \rangle$	1.471
O11	1.336(13)	B10 tetrahedron	
O18	1.381(13)	O12	1.464(13)
O4	1.393(13)	O17	1.465(13)
$\langle \text{B2-O} \rangle$	1.370	O5	1.476(13)
B3 triangle		O13	1.478(13)
O10	1.343(13)	$\langle \text{B10-O} \rangle$	1.471
O15	1.367(14)	B7 triangle	
O8	1.387(13)	O3	1.333(14)
$\langle \text{B3-O} \rangle$	1.366	O6	1.367(14)
B5 triangle		O8	1.378(13)
O5	1.357(13)	$\langle \text{B7-O} \rangle$	1.359
O7	1.376(13)	B8 triangle	
O6	1.376(13)	O12	1.349(13)
$\langle \text{B5-O} \rangle$	1.370	O16	1.355(13)
B6 triangle		O7	1.380(13)
O17	1.355(12)	$\langle \text{B8-O} \rangle$	1.361
O18	1.367(12)	B9 triangle	
O1	1.384(13)	O2	1.349(14)
$\langle \text{B6-O} \rangle$	1.369	O9	1.359(13)
		O4	1.389(14)
		$\langle \text{B9-O} \rangle$	1.366

refined coordinates of basis atoms and the interatomic distances calculated on their basis are given in Tables 2–4. The calculation of the bond-valence sum, in which the algorithm and parameters proposed in

[16, 17] were used, confirmed the presence of OH and H_2O groups. The solved crystal structure of the novel cesium pentaborate is described by the crystallochemical formula $\text{Cs}[\text{B}_5\text{O}_7(\text{OH})_2] \cdot 0.5\text{H}_2\text{O}$.

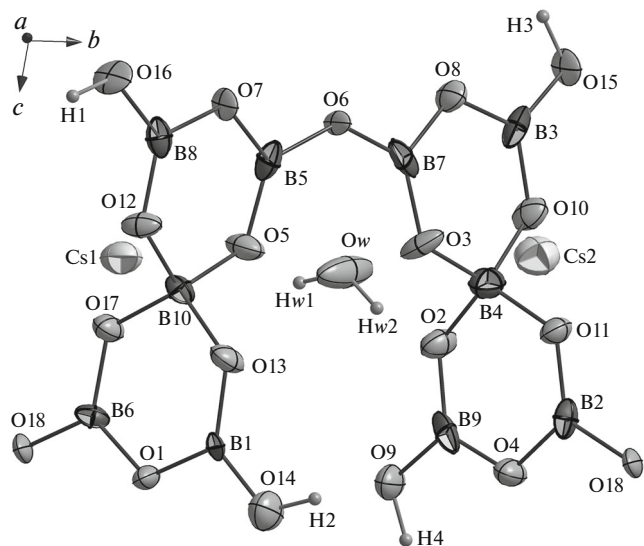
Table 4. Geometric characteristics of hydrogen bonds in the $\text{Cs}[\text{B}_5\text{O}_7(\text{OH})_2] \cdot 0.5\text{H}_2\text{O}$ structure

$D\text{--}H\cdots A$	Distance, Å			Angle $D\text{--}H\cdots A$, deg
	$D\text{--}H$	$H\cdots A$	$D\cdots A$	
$\text{O16--H1}\cdots\text{O15}$	0.900(2)	1.88(3)	2.749(10)	160(8)
$\text{O14--H2}\cdots\text{O9}$	0.900(2)	2.03(5)	2.873(10)	156(12)
$\text{O15--H3}\cdots\text{Ow2}$	0.900(2)	1.84(4)	2.695(11)	158(9)
$\text{O9--H4}\cdots\text{O5}$	0.900(2)	2.36(7)	3.178(10)	152(13)
$\text{Ow--Hw1}\cdots\text{O13}$	0.900(2)	1.90(6)	2.736(10)	153(13)
$\text{Ow--Hw2}\cdots\text{O2}$	0.900(2)	1.85(3)	2.734(11)	165(9)

ANALYSIS OF INTERATOMIC DISTANCES AND CRYSTAL STRUCTURE DESCRIPTION

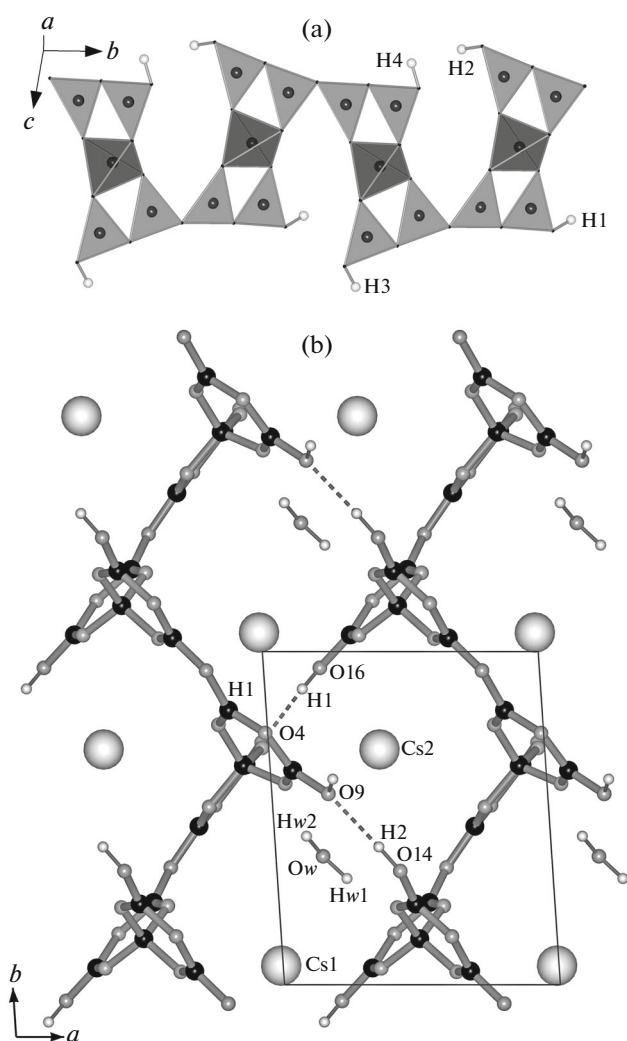
The study of the crystal structure of novel cesium pentaborate $\text{Cs}[\text{B}_5\text{O}_7(\text{OH})_2] \cdot 0.5\text{H}_2\text{O}$ confirmed that it is isostructural with the previously investigated rubidium- [3] and ammonium-containing analogs [4]; for this reason, the interatomic distances were analyzed by comparing data on these three compounds.

An independent fragment of cesium pentaborate crystal structure is shown in Fig. 1. Boron atoms occupy 10 unique sites, two of which have tetrahedral coordination with respect to oxygen and eight are characterized by triangular coordination. The B–O distance in triangles varies within 1.333(14)–1.396(13) Å, with a somewhat smaller spread of values in comparison with the rubidium analogue (1.332–1.409 Å) and somewhat larger spread in comparison with ammonium-containing pentaborate (1.337–1.391 Å). The

**Fig. 1.** Coordination of cations in the $\text{Cs}[\text{B}_5\text{O}_7(\text{OH})_2] \cdot 0.5\text{H}_2\text{O}$ crystal structure by an example of independent fragment; the thermal ellipsoids of the atoms are drawn at the 80% probability level.

boron tetrahedron is practically undistorted. The B–O distances are typical of boron in the tetrahedral coordination and lie in the ranges of 1.465(14)–1.478(13) and 1.464(13)–1.478(13) Å for B1 and B2, respectively, with an average value of 1.471 Å for both tetrahedra. The average B–O distance somewhat exceeds the corresponding value of 1.469(4) Å for the NH_4 -analogue. Note that borate tetrahedra are more strongly distorted in the structure of rubidium analogue and exhibit a larger spread of B–O distances: 1.465–1.503 Å.

Double pentaborate fragments, with two oxygen atoms shared, form a zigzag ribbon elongated along the [010] direction (Fig. 2a). The dangling vertices of BO_3 triangles in these ribbons are protonated and form hydroxyl groups O16–H1, O14–H2, O15–H3, and

**Fig. 2.** Fragment of the $\text{Cs}[\text{B}_5\text{O}_7(\text{OH})_2] \cdot 0.5\text{H}_2\text{O}$ crystal structure: (a) pentaborate chain, elongated along the [010] direction, and (b) layer of pentaborate chains linked by hydrogen bonds, oriented parallel to the ab plane, and containing cesium cations and water molecules.

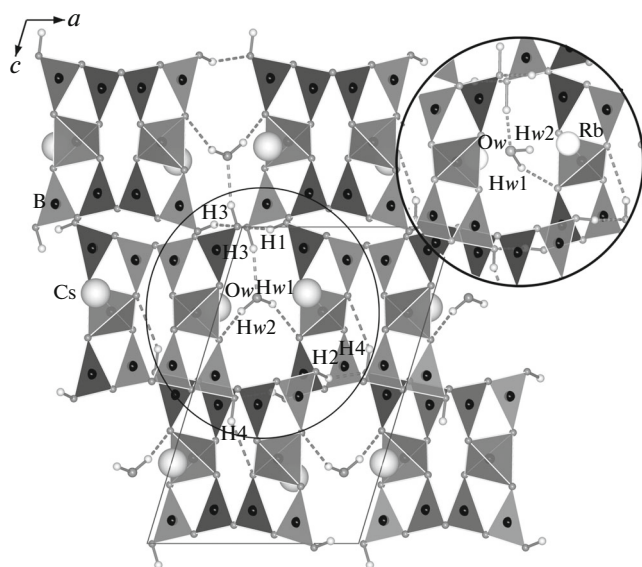


Fig. 3. Projection of the $\text{Cs}[\text{B}_5\text{O}_7(\text{OH})_2] \cdot 0.5\text{H}_2\text{O}$ crystal structure on the xz plane. The inset shows the configuration of water molecule in the $\text{Rb}[\text{B}_5\text{O}_7(\text{OH})_2] \cdot 0.5\text{H}_2\text{O}$ crystal structure.

$\text{O}_9\text{--H}_4$. The $\text{O}_{16}\text{--H}_1$ and $\text{O}_{14}\text{--H}_2$ groups play the role of donors, being involved in hydrogen bonding with oxygen atoms O_{15} and O_9 from neighboring pentaborate ribbons, as a result of which polar layers alternating along the c axis are formed (Fig. 2b). The water molecule, being located in the voids of pentaborate ribbon layer, serves as a donor for two hydrogen bonds with oxygen atoms O_2 and O_{13} , which are shared by boron tetrahedra and triangles of neighboring ribbons (Fig. 3). The acceptor function of this water molecule O_w is implemented due to its participation in the hydrogen bond with the $\text{H}_3\text{--O}_{15}$ hydroxyl group, coordinated with a boron atom B_3 from a neighboring-layer ribbon (Fig. 3). Thus, the water molecule reinforces the pentaborate ribbon layer and links it with one of the two neighboring layers. Due to the polarity of the layer under consideration, it is linked with the other (opposite) layer via a hydrogen bond between the hydroxyl group $\text{H}_4\text{--O}_9$ and oxygen atoms O_5 . According to Table 4, the hydrogen bond formed

by H_4 is the weakest one; all others can be considered as average. In comparison with the rubidium analogue [3], the position of the hydrogen atom H_w2 of the water molecule in the crystal structure of the compound under study was found to differ (Fig. 3, inset). The water molecule in this structure is fixed in the void by three hydrogen bonds: $\text{O}_w\text{--H}_w1\cdots\text{O}_{13}$, $\text{O}_w\text{--H}_w2\cdots\text{O}_2$, and $\text{O}_{15}\text{--H}_3\cdots\text{O}_2$. At the same time, two hydrogen bonds are observed in $\text{Rb}[\text{B}_5\text{O}_7(\text{OH})_2] \cdot 0.5\text{H}_2\text{O}$: $\text{H}_w2\text{--O}_w\cdots\text{O}_{11}$ and $\text{O}_5\text{--H}_2\cdots\text{O}_w$. The water molecule atoms in the structure of ammonium analogue are distributed over two sites; the hydrogen bond topology is similar to that in the compound under consideration.

Cesium cations occupy two independent sites, being located in the space between pentaborate chains (Figs. 2, 3), and are surrounded by nine nearest oxygen atoms (Fig. 1). The $\text{Cs}1\text{--O}$ and $\text{Cs}2\text{--O}$ distances vary in the ranges of $2.927(7)\text{--}3.486(7)$ Å (average 3.204 Å) and $3.066(8)\text{--}3.481(10)$ Å (average 3.282 Å), respectively. These values are systematically increased in comparison with the $\text{Rb}1\text{--O}$ and $\text{Rb}2\text{--O}$ distances (average values 3.085 and 3.188 Å) in the rubidium pentaborate crystal structure.

It is natural that the increase in the ionic radius of alkaline cation, $\text{NH}_4 \rightarrow \text{Rb} \rightarrow \text{Cs}$, in the series of $A[\text{B}_5\text{O}_7(\text{OH})_2] \cdot 0.5\text{H}_2\text{O}$ compounds leads to an increase in their unit-cell volumes (Table 5). The parameters a and c increase as well, whereas the parameter b varies only slightly for all terms of this series. This is related to the rigidity of the main structural fragment in the compounds under consideration: pentaborate chains, elongated along the crystallographic axis b .

It was shown in [3, 4] that isostructural compounds $A[\text{B}_5\text{O}_7(\text{OH})_2] \cdot 0.5\text{H}_2\text{O}$ ($A = \text{NH}_4, \text{Rb}$) are related to the mineral larderellite $\text{NH}_4[\text{B}_5\text{O}_7(\text{OH})_2] \cdot \text{H}_2\text{O}$, because the crystal structures of both types are based on zigzag pentaborate chains, elongated along the b axis. The main differences in the structure types under consideration are related to the configuration and topology of mutual arrangement of the aforementioned chain fragments and the character of filling voids between them. In the larderellite structure,

Table 5. Crystallographic characteristics of isostructural compounds described by the general formula $A[\text{B}_5\text{O}_7(\text{OH})_2] \cdot 0.5\text{H}_2\text{O}$ ($A = \text{NH}_4, \text{Rb}, \text{Cs}$)

A	$a, \text{Å } \alpha, \text{ deg}$	$b, \text{Å } \beta, \text{ deg}$	$c, \text{Å } \gamma, \text{ deg}$	$V, \text{Å}^3$	References
NH_4	7.6207(15)	9.2328(18)	11.926(2)	793.8(3)	[4]
	99.46 (3)	105.89 (3)	91.54 (3)		
Rb	7.679(4)	9.253(6)	12.053(9)	808(2)	[3]
	98.55(5)	106.80(5)	91.71(5)		
Cs	7.8107(5)	9.1929(8)	12.3553(11)	839.1(1)	This study
	98.98(1)	106.32(1)	91.10(1)		

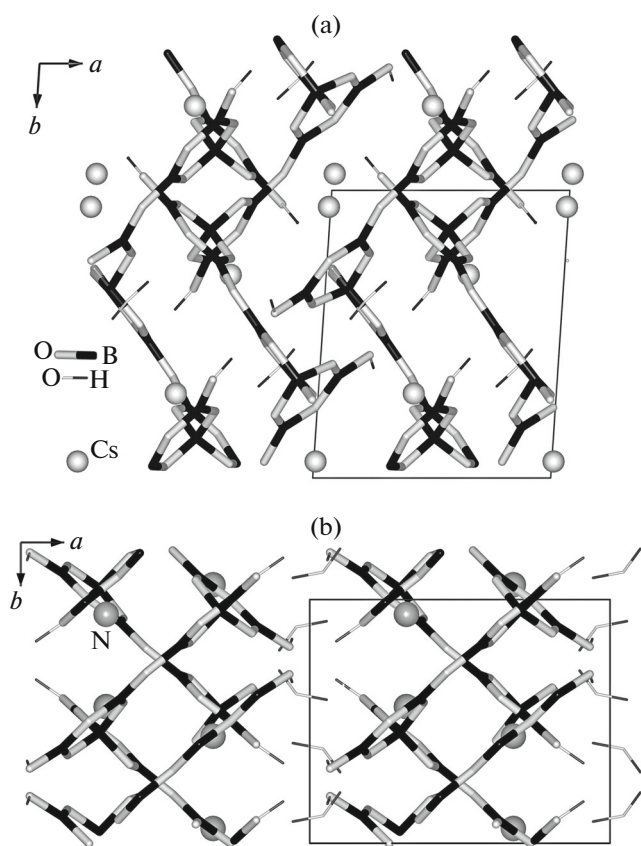


Fig. 4. Projection of pentaborate chains on the xy plane in the (a) $\text{Cs}[\text{B}_5\text{O}_7(\text{OH})_2] \cdot 0.5\text{H}_2\text{O}$ and (b) $\text{NH}_4[\text{B}_5\text{O}_7(\text{OH})_2] \cdot \text{H}_2\text{O}$ crystal structures.

neighboring pentaborate blocks $[\text{B}_5\text{O}_{10}]$ in a chain are symmetrically linked by a screw twofold axis. In the structures of synthetic pentaborates, the symmetrically independent element is the double pentaborate fragment $[\text{B}_{10}\text{O}_{20}]$. The chains linked by the twofold axis are intercrossed along the b axis in the larderellite unit cell (Fig. 4b). In the $A[\text{B}_5\text{O}_7(\text{OH})_2] \cdot 0.5\text{H}_2\text{O}$ ($A = \text{NH}_4, \text{Rb}, \text{Cs}$) structures, similar chains, multiplied by the inversion center, have a parallel orientation (Fig. 4a). For this reason, layers alternating along the $[001]$ direction are present in the larderellite structure; they are perpendicular to the a axis, and the space between them is occupied by water molecules. This arrangement determines the lamellar habit of crystals along the $[100]$ direction. This extensive space is absent in the crystal structure of synthetic pentaborates (Fig. 3, 4). Due to the decrease in the number of water molecules by half (in comparison with larderelite), mutual displacement of pentaborate chains in the ab plane, and their additional reinforcement by

hydrogen bonds, the closest packed layers are oriented perpendicular to the $[010]$ direction (Fig. 3). This configuration is in agreement with the tabular shape of crystals of the compound under study; it was established that their flattened shape is related to the development of $[010]$ faces. Tabular shape was also described for ammonium-containing pentaborate crystals [4]. The observed isometric habit of crystals of the analogue $\text{Rb}[\text{B}_5\text{O}_7(\text{OH})_2] \cdot 0.5\text{H}_2\text{O}$ [3] may be related to their growth conditions, for example, growth under supersaturation.

ACKNOWLEDGMENTS

We are grateful to V.O. Yapaskurt for the X-ray spectroscopic analysis of the sample and to N. V. Zubkova for carrying out the X-ray experiment.

This study was supported by the Russian Foundation for Basic Research, project no. 18-03-00908.

REFERENCES

1. H. Behm, *Acta Crystallogr. C* **40**, 1114 (1984).
2. N. Penin, L. Seguin, B. Gerand, et al., *J. Alloys Compd.* **334**, 97 (2002).
3. E. L. Belokoneva, T. A. Borisova, and O. V. Dimitrova, *Crystallogr. Rep.* **48** (4), 583 (2003).
4. L. Y. Li, G. B. Li, M. Xiong, et al., *Acta Crystallogr. C* **59** (11), 1115 (2003).
5. S. Merlino and F. Sartori, *Acta Crystallogr. B* **25** (11), 2264 (1969).
6. S. Merlino, *Acta Crystallogr. B* **28** (12), 3559 (1972).
7. S. Merlino and F. Sartori, *Contrib. Mineral. Petrol.* **27** (2), 159 (1970).
8. S. Merlino and F. Sartori, *Science* **171** (3969), 377 (1971).
9. R. Thomas, P. Davidson, and A. Hahn, *Am. Mineral.* **93** (7), 1034 (2008).
10. V. G. Dmitriev, G. G. Gurzadyan, and D. N. Nikogosyan, *Handbook of Nonlinear Optical Crystals* (Springer, Berlin, 1997), p. 67.
11. P. Becker, P. Held, and L. Bohaty, *Cryst. Res. Technol.* **35**, 1251 (2000).
12. *CrysAlisPro. CrysAlis Software System* (Oxford Diffraction, Abingdon, UK, 2007).
13. L. J. Farrugia, *J. Appl. Crystallogr.* **32**, 837 (1999).
14. E. Prince, *International Tables for Crystallography* (IUCr, 2004), Tables 4.2.6.8; 6.1.14.
15. G. M. Sheldrick, *Acta Crystallogr. C* **71**, 3 (2015).
16. I. D. Brown and D. Altermatt, *Acta Crystallogr. B* **41**, 244 (1986).
17. I. D. Brown, *Chem. Rev.* **109**, 6858 (2009).

Translated by Yu. Sin'kov